

Relativistic approach to $(e, e'p)$ and (e, e') reactions

Andrea Meucci,¹ Carlotta Giusti,¹ and Franco Davide Pacati¹

¹*Dipartimento di Fisica Nucleare e Teorica, Università di Pavia and
Istituto Nazionale di Fisica Nucleare, Sezione di Pavia, I-27100 Pavia, Italy*

A relativistic distorted wave impulse approximation model for electron-induced one proton knockout reactions and a Green's function approach to inclusive scattering are developed. Results for $(e, e'p)$ and (e, e') reactions are presented in various kinematical conditions and compared (when possible) with nonrelativistic calculations.

PACS numbers: 25.30.Fj: Inelastic electron scattering to continuum, 25.20.Lj: Photoproduction reactions, 24.10.Jv: Relativistic models, 24.10.Eq: Coupled-channel and distorted-wave models, 24.10.Cn: Many-body theory

1. INTRODUCTION

A long series of high-precision experiments on several nuclei [1–7] have generated a well established tradition which singles out exclusive $(e, e'p)$ knockout reactions as the primary tool to explore the single-particle aspects of the nucleus. Theoretical calculations were carried out within the framework of a nonrelativistic distorted wave impulse approximation (DWIA), where final-state interactions (FSI) and Coulomb distortion of the electron wave functions are taken into account [8]. Phenomenological ingredients were used to compute bound and scattering states. This approach was able to describe to a high degree of accuracy the shape of the experimental momentum distribution for several nuclei in a wide range of different kinematics [9, 10]. However, a systematic rescaling of the normalization of the bound state, interpreted as the spectroscopic factor for the corresponding level, had to be applied in order to reproduce the magnitude of the experimental distribution.

Similar models based on a fully relativistic DWIA (RDWIA) framework were developed in more recent years. The Dirac equation is solved directly for the nucleon bound and scattering states [11–13] or, equivalently, a Schrödinger-like equation is solved and the spinor distortion by the Dirac scalar and vector potentials is incorporated in an effective current operator in the so-called effective Pauli reduction [14–16].

A successful description of new $(e, e'p)$ data at higher momentum transfer from Jefferson Laboratory (JLab) [17, 18] has been achieved within the framework of RDWIA, but slightly different spectroscopic factors are deduced, because the relativistic optical potentials in general give a stronger absorption than the corresponding nonrelativistic ones [13, 19]. Moreover, the limits of validity of the nonrelativistic DWIA analysis versus RDWIA were not always properly explored, as discussed in Ref. [16], resulting, e.g., in a certain degree of ambiguity for the spectroscopic factors extracted at low energy.

In Sec. 2 a RDWIA approach to low- and high-energy $(e, e'p)$ data is presented and a careful analysis of the limits of the nonrelativistic DWIA is carried out. The sensitivity to different off-shell prescriptions for the electromagnetic current operator will also be discussed [20, 21].

In Sec. 3 a Green's function approach for the inclusive electron scattering is developed [22]. In the inclusive (e, e') scattering only the scattered electron is detected whereas the final nuclear state is not determined. The one-body mechanism is assumed to give the main contribution to the reaction in the quasielastic region. However, when the experimental data of the separation between the longitudinal and transverse responses became available it was clear that a more complicated framework than the single-particle model coupled to one-nucleon knockout was necessary. A review till 1995 of the experimental data and their possible explanations is given in Ref. [9]. Thereafter, only a few experimental papers were published [23, 24]. New experiments with high experimental resolution are planned at JLab [25] in order to extract the response functions.

From the theoretical side, a wide literature was produced in order to explain the main problems raised by the separation, i.e., the lack of strength in the longitudinal response and the excess of strength in the transverse one. The more recent papers are mainly concerned with the contribution to the inclusive cross section of meson exchange currents and isobar excitations [26–28], with the effect of correlations [29, 30], and the use of a relativistic framework in the calculations [28].

At present, however, the experimental data are not yet completely understood. A possible solution could be the combined effect of two-body currents and tensor correlations [29, 31, 32].

In our Green’s function approach to (e, e') scattering the spectral representation of the single particle Green function, based on a biorthogonal expansion in terms of the eigenfunctions of the nonhermitian optical potential, allows one to perform explicit calculations and to treat final state interactions consistently in the inclusive and in the exclusive reactions.

2. THE $(e, e'p)$ REACTION

A. Relativistic current

The main ingredient of the calculation is the nuclear transition amplitude, i.e.,

$$J^\mu = \int d\mathbf{r} \bar{\chi}^{(-)}(\mathbf{r}) \hat{j}^\mu \exp\{i\mathbf{q} \cdot \mathbf{r}\} \varphi(\mathbf{r}) . \quad (1)$$

In RDWIA it is calculated using relativistic wave functions for initial and final states.

The bound state wave function, φ , is given by the Dirac-Hartree solution of a relativistic Lagrangian containing scalar and vector potentials deduced in the context of a relativistic mean field theory that satisfactorily reproduces single-particle properties of several spherical and deformed nuclei [33].

The ejectile wave function, $\chi^{(-)}$, is written in terms of its positive energy component Ψ_{f+} following the direct Pauli reduction method

$$\chi^{(-)} = \left(\begin{array}{c} \chi_+ \\ \frac{\boldsymbol{\sigma} \cdot \mathbf{p}'}{M + E' + S - V} \chi_+ \end{array} \right) , \quad (2)$$

where $S = S(r)$ and $V = V(r)$ are the scalar and vector potentials for the nucleon with energy E' [34]. The upper component χ_+ is related to a Schrödinger equivalent wave function Φ_f by the Darwin factor $D(r)$, i.e.,

$$\chi_+ = \sqrt{D(r)} \Phi_f , \quad D(r) = \frac{M + E' + S - V}{M + E'} . \quad (3)$$

Φ_f is a two-component wave function which is solution of a Schrödinger equation containing equivalent central and spin-orbit potentials obtained from the scalar and vector potentials.

The choice of the electromagnetic operator is a longstanding problem. Here we discuss the three current conserving expressions [15, 35]

$$\begin{aligned} \hat{j}_{cc1}^\mu &= G_M(Q^2) \gamma^\mu - \frac{\kappa}{2M} F_2(Q^2) \bar{P}^\mu , \\ \hat{j}_{cc2}^\mu &= F_1(Q^2) \gamma^\mu + i \frac{\kappa}{2M} F_2(Q^2) \sigma^{\mu\nu} q_\nu , \\ \hat{j}_{cc3}^\mu &= F_1(Q^2) \frac{\bar{P}^\mu}{2M} + \frac{i}{2M} G_M(Q^2) \sigma^{\mu\nu} q_\nu , \end{aligned} \quad (4)$$

where $q^\mu = (\omega, \mathbf{q})$ is the four-momentum transfer, $Q^2 = |\mathbf{q}|^2 - \omega^2$, $\bar{P}^\mu = (E + E', \mathbf{p}_m + \mathbf{p}')$, κ is the anomalous part of the magnetic moment, F_1 and F_2 are the Dirac and Pauli nucleon form factors, $G_M = F_1 + \kappa F_2$ is the Sachs nucleon magnetic form factor, and $\sigma^{\mu\nu} = (i/2) [\gamma^\mu, \gamma^\nu]$. These expressions are equivalent for on-shell particles thanks to Gordon identity. However, since nucleons in the nucleus are off-shell we expect that these formulas should give different results. Current conservation is restored by replacing the longitudinal current and the bound nucleon energy by [35]

$$J^L = J^z = \frac{\omega}{|\mathbf{q}|} J^0 , \quad E = \sqrt{|\mathbf{p}_m|^2 + M^2} = \sqrt{|\mathbf{p}' - \mathbf{q}|^2 + M^2} . \quad (5)$$

B. Nonrelativistic current

In nonrelativistic DWIA the transition amplitude of Eq. (1) is evaluated using eigenfunctions of a Schrödinger equation for both the bound and scattering states. In standard DWIA analyses phenomenological ingredients are usually adopted. In this work and in order to perform a consistent comparison with RDWIA calculations, we employ for the bound state the upper component of the Dirac wave function φ and for the final state the Schrödinger-like wave function Φ_f .

The nuclear current operator is obtained from the Foldy-Wouthuysen reduction of the free-nucleon Dirac current through an expansion in a power series of $1/M$. Performing the expansion through second order we get

$$\begin{aligned} j_{(0)}^0 &= F_1 \quad , \quad j_{(1)}^0 = 0 \quad , \quad j_{(2)}^0 = \frac{(F_1 + 2\kappa F_2)}{8M^2} (-Q^2 - i\boldsymbol{\sigma} \cdot \mathbf{P} \times \mathbf{q}) \quad , \\ j_{(0)} &= 0 \quad , \quad j_{(1)} = \frac{(F_1 + \kappa F_2)}{2M} i\boldsymbol{\sigma} \times \mathbf{q} + \frac{1}{2M} F_1 \mathbf{P} \quad , \quad j_{(2)} = -\frac{(F_1 + 2\kappa F_2)}{8M^2} i\boldsymbol{\omega} \boldsymbol{\sigma} \times \mathbf{P} \quad . \end{aligned} \quad (6)$$

C. The $(e, e'p)$ cross section

The coincidence cross section of the $(e, e'p)$ reaction can be written as the contraction between the lepton tensor, completely determined by quantum electrodynamics, and the hadron tensor, whose components are given by suitable bilinear combinations of the nuclear transition amplitude in Eq. (1). In case of unpolarized reactions the cross section can be written in terms of four response functions, $R_{\lambda\lambda'}$, as

$$\sigma = K \{v_L R_L + v_T R_T + v_{LT} R_{LT} \cos(\vartheta) + v_{TT} R_{TT} \cos(2\vartheta)\} \quad , \quad (7)$$

where K is a kinematic factor, and ϑ is the out-of-plane angle between the electron scattering plane and the $(\mathbf{q}, \mathbf{p}')$ plane. The coefficients $v_{\lambda\lambda'}$ are obtained from the lepton tensor components and depend only upon the electron kinematics [9, 10]. The response functions are defined as

$$\begin{aligned} R_L &\propto \langle J^0 (J^0)^\dagger \rangle \quad , \quad R_T \propto \langle J^x (J^x)^\dagger \rangle + \langle J^y (J^y)^\dagger \rangle \quad , \\ R_{LT} &\propto -2 \operatorname{Re} \left[\langle J^x (J^0)^\dagger \rangle \right] \quad , \quad R_{TT} \propto \langle J^x (J^x)^\dagger \rangle - \langle J^y (J^y)^\dagger \rangle \quad , \end{aligned} \quad (8)$$

where average over the initial and sum over the final states is performed fulfilling energy conservation. In our frame of reference the z axis is along \mathbf{q} , and the y axis is parallel to $\mathbf{q} \times \mathbf{p}'$.

If the electron beam is longitudinally polarized with helicity h , the coincidence cross section for a knocked out nucleon with spin directed along $\hat{\mathbf{s}}$ can be written as

$$\sigma_{h, \hat{\mathbf{s}}} = \frac{1}{2} \sigma \left[1 + \mathbf{P} \cdot \hat{\mathbf{s}} + h \left(A + \mathbf{P}' \cdot \hat{\mathbf{s}} \right) \right] \quad , \quad (9)$$

where σ is the unpolarized cross section of Eq. (7), \mathbf{P} the induced polarization, A the electron analyzing power and \mathbf{P}' the polarization transfer coefficient. We choose for the polarimeter the three perpendicular directions: \mathbf{L} parallel to \mathbf{p}' , \mathbf{N} along $\mathbf{q} \times \mathbf{p}'$, and $\mathbf{T} = \mathbf{N} \times \mathbf{L}$.

D. Results and Discussion

In Fig. 1 the unpolarized $^{16}\text{O}(e, e'p)$ reaction leading to the $p_{1/2}$ ground state and the $p_{3/2}$ first excited state of ^{15}N is considered. In the left panel, data have been collected at NIKHEF in parallel kinematics at a constant proton energy of 90 MeV in the center-of-mass system [7]. They are presented in the form of the reduced cross section [9]. The results for the transition to the $p_{1/2}$ ground state have been multiplied by 40. The dot-dashed lines refer to the nonrelativistic

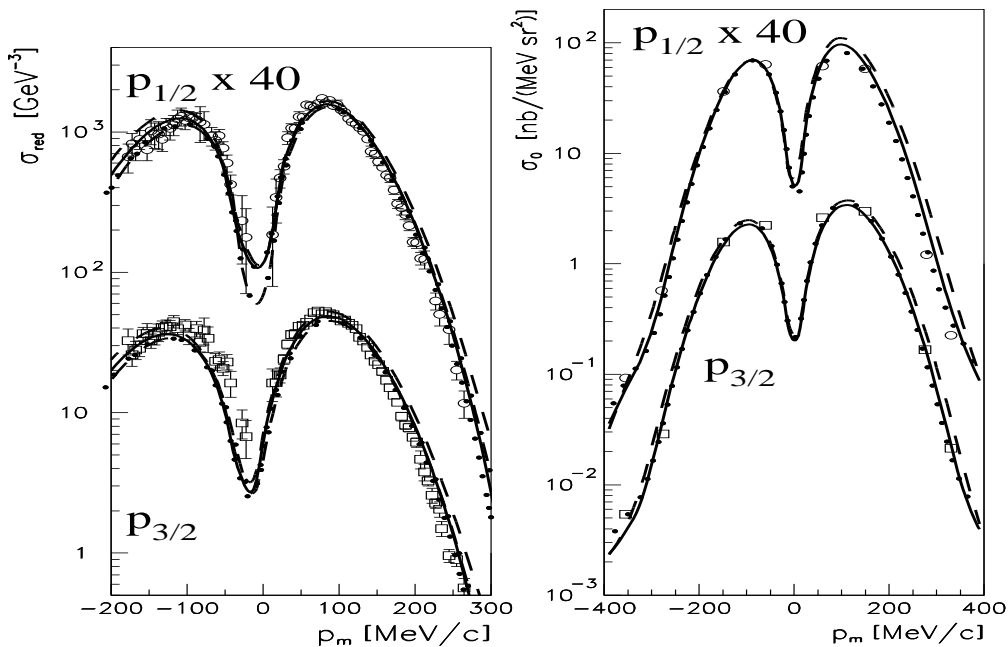


FIG. 1: Left panel: reduced cross section for the $^{16}\text{O}(e, e'p)^{15}\text{N}$ transition to the $p_{1/2}$ ground state and $p_{3/2}$ first excited state of ^{15}N at $E_p = 90$ MeV constant proton energy in the center-of-mass system in parallel kinematics [7]. Right panel: cross section for the same reaction but at $Q^2 = 0.8$ $(\text{GeV}/c)^2$ in constant (\mathbf{q}, ω) kinematics [17]. Data for the $p_{1/2}$ state have been multiplied by 40. Dashed, solid, and dotted lines represent the results of the RDWIA approach with cc1, cc2, cc3 off-shell prescriptions, respectively. Dot-dashed lines in the left panel are the nonrelativistic results.

calculations of Sec. 2B. The theoretical results have been rescaled in order to reproduce the data by applying the spectroscopic factors $Z_{p_{1/2}} = 0.64$ and $Z_{p_{3/2}} = 0.54$, respectively. The solid lines show the results of the RDWIA analysis with the cc2 off-shell prescription; dashed and dotted lines indicate the results when using the cc1 and cc3 recipes, respectively. The resulting spectroscopic factors, $Z_{p_{1/2}} = 0.708$ and $Z_{p_{3/2}} = 0.602$, have been obtained by a χ^2 fit using the cc3 current [21], which gives an overall better description of the $(e, e'p)$ observables. Only small differences are found between the relativistic and the nonrelativistic models. Thus, they are almost equivalent in comparison with the data, which are reasonably described by both calculations.

In the right panel, the same reaction is considered at the JLab constant (\mathbf{q}, ω) kinematics with $Q^2 = 0.8$ $(\text{GeV}/c)^2$ [17]. The data now refer to the differential unpolarized cross section. The $p_{1/2}$ results are multiplied by a factor 40. The theoretical curves have the same meaning as in the left panel and are rescaled again by the same spectroscopic factors. Only RDWIA calculations are shown since at the proton energy of this experiment relativistic effects are large and a nonrelativistic analysis gives unreliable results. The agreement with the data is very good also in this case. This outcome is particularly welcome, since the spectroscopic factors correspond to a nuclear property that must be independent of Q^2 .

In Fig. 2 the response functions measured at JLab in the same kinematics with $Q^2 = 0.8$ $(\text{GeV}/c)^2$ [17] are displayed and compared with our RDWIA calculations. The agreement with the data is satisfactory and of about the same quality as in other relativistic analyses [13, 15], but for the R_{LT} response function, where only the cc3 calculation reproduces the $p_{1/2}$ data at low missing momentum while the cc2 one better reproduces the $p_{3/2}$ data. In Fig. 3 the polarization transfer components P'^L, P'^T are shown as functions of the missing momentum p_m for the $^{16}\text{O}(\vec{e}, e'\vec{p})$ reaction at $Q^2 = 0.8$ $(\text{GeV}/c)^2$ and constant (\mathbf{q}, ω) for the transitions to the ^{15}N $p_{1/2}, p_{3/2}$, and

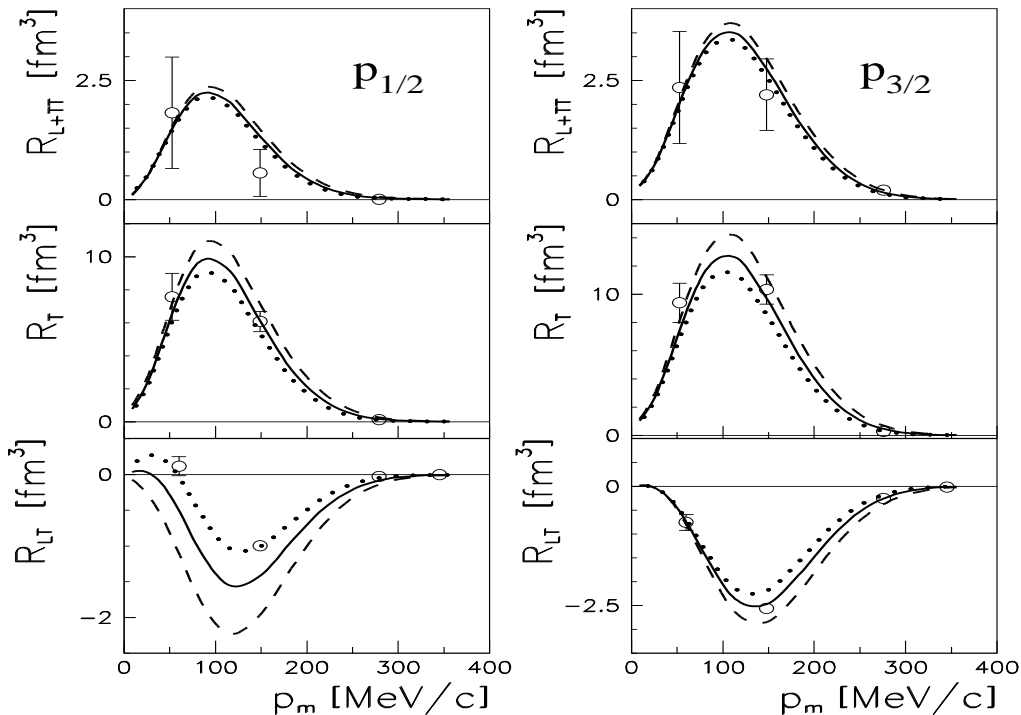


FIG. 2: Response functions for the $^{16}\text{O}(e, e'p)$ reaction at $Q^2 = 0.8$ $(\text{GeV}/c)^2$ in constant (\mathbf{q}, ω) kinematics [18] leading to the ^{15}N $p_{1/2}$ (left column) and $p_{3/2}$ (right column) residual states. Line convention as in Fig. 1

$s_{1/2}$, respectively [18]. For these observables and in this kinematics, the sensitivity to off-shell effects is at most $\lesssim 15\%$. The overall agreement with the data is still good.

As a first step to study the role of meson exchange currents (MEC), we have considered in Ref. [36] the contribution due to the seagull diagram. The seagull current is written in momentum space as in Refs. [37, 38] and with the cutoff $\Lambda = 1250$ MeV in the pion propagator. The inclusion of the seagull diagram enhances the RDWIA results, but, in contrast to (γ, p) scattering, the effects are generally small and visible only at high missing momenta. Thus, the comparison with data, that were already well reproduced by the direct knock-out model, is practically unaffected. In particular, no significant effects were obtained on the polarization observables from MIT-Bates on $^{12}\text{C}(e, e'\vec{p})^{11}\text{B}$ [39] and from JLab on $^{16}\text{O}(\vec{e}, e'\vec{p})^{15}\text{N}$ [18] reactions.

3. THE (e, e') REACTION

In the one photon exchange approximation the inclusive cross section for the quasielastic (e, e') scattering on a nucleus is given in terms of two response functions as [9]

$$\sigma_{inc} = K (2\varepsilon_L R_L + R_T) , \quad (10)$$

where K is a kinematical factor and

$$\varepsilon_L = \frac{Q^2}{q^2} \left(1 + 2 \frac{q^2}{Q^2} \tan^2(\vartheta_e/2) \right)^{-1} \quad (11)$$

measures the polarization of the virtual photon. In Eq. (11) ϑ_e is the scattering angle of the electron. The longitudinal and transverse response functions, R_L and R_T , contain all nuclear

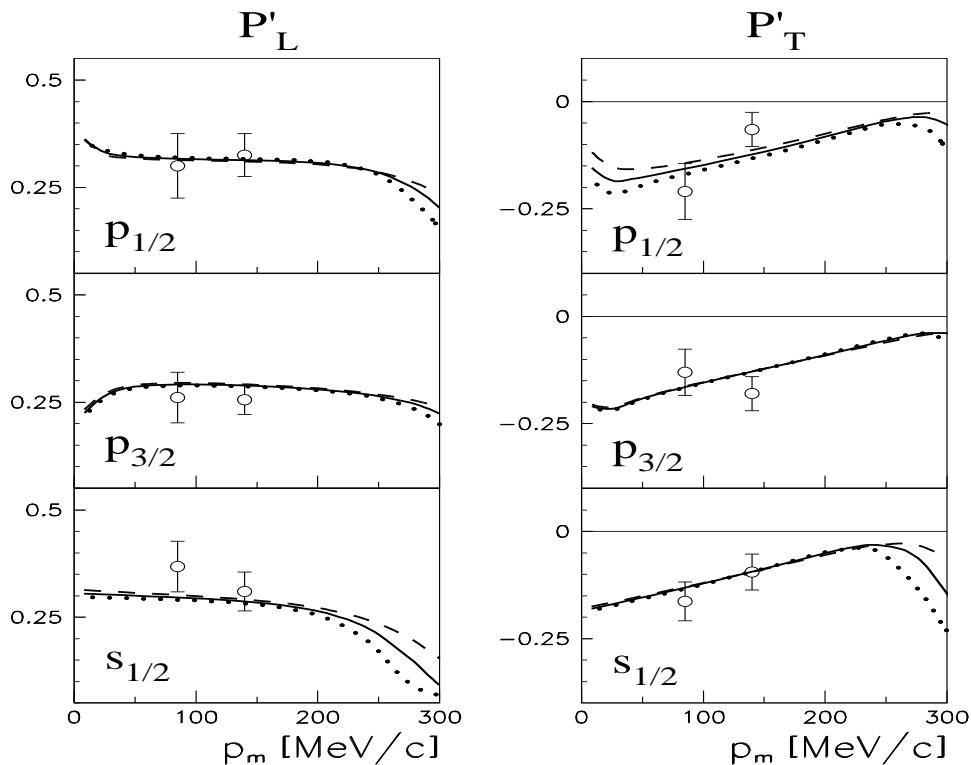


FIG. 3: Polarization transfer components P'^L, P'^T for the $^{16}\text{O}(\vec{e}, e'\vec{p})$ reaction at $Q^2 = 0.8 \text{ (GeV}/c)^2$ in constant (\mathbf{q}, ω) kinematics [18] leading to the ^{15}N $p_{1/2}, p_{3/2}$ and $s_{1/2}$ residual states. Line convention as in Fig. 1.

structure information and are defined as in Eq. (8). They are directly related to the hadron tensor components

$$W^{\mu\mu}(\omega, q) = \sum_f |\langle \Psi_f | J_N^\mu(\mathbf{q}) | \Psi_0 \rangle|^2 \delta(E_0 + \omega - E_f) = -\frac{1}{\pi} \text{Im} \langle \Psi_0 | J_N^{\mu\dagger}(\mathbf{q}) G(E_f) J_N^\mu(\mathbf{q}) | \Psi_0 \rangle. \quad (12)$$

Here J_N^μ is the nuclear charge-current operator which connects the initial state $|\Psi_0\rangle$ of the nucleus, of energy E_0 , with the final states $|\Psi_f\rangle$, of energy E_f , both eigenstates of the $(A+1)$ -body Hamiltonian H . The sum runs over the scattering states corresponding to all of the allowed asymptotic configurations and includes possible discrete states. $G(E_f)$ is the Green function related to H , i.e.,

$$G(E_f) = \frac{1}{E_f - H + i\eta}. \quad (13)$$

Here and in all the equations involving G the limit for $\eta \rightarrow +0$ is understood. It must be performed after calculating the matrix elements between normalizable states.

In Ref. [22] we have showed that the spectral representation of the single particle Green's functions related to the optical potential allows practical calculations of the hadron tensor components for the inclusive (e, e') scattering. Here, we briefly recall the most important points of the method, without discussing in details the approximations involved. Assuming only one-body terms in the nuclear current, Eq. (12) can be reduced to a single-particle expression whose self-energy is the

Feshbach’s optical potential [22]. We then perform a biorthogonal expansion of the full particle-hole Green’s function in terms of the eigenfunctions the optical potential, \mathcal{V} , and its Hermitian conjugate, \mathcal{V}^\dagger , i.e.,

$$[\mathcal{E} - T - \mathcal{V}^\dagger(E)] | \chi_{\mathcal{E}}^{(-)}(E) \rangle = 0 \quad , \quad [\mathcal{E} - T - \mathcal{V}(E)] | \tilde{\chi}_{\mathcal{E}}^{(-)}(E) \rangle = 0 . \quad (14)$$

Note that \mathcal{E} and E are not necessarily the same. The spectral representation is

$$\mathcal{G}(E) = \int_M^\infty d\mathcal{E} | \tilde{\chi}_{\mathcal{E}}^{(-)}(E) \rangle \frac{1}{E - \mathcal{E} + i\eta} \langle \chi_{\mathcal{E}}^{(-)}(E) | , \quad (15)$$

and the hadron tensor can be written in an expanded version in terms of the single-particle wave function, $|\varphi_n\rangle$, of the initial state, corresponding to the energy ε_n and whose spectral strength is λ_n , as

$$W^{\mu\mu}(\omega, q) = -\frac{1}{\pi} \sum_n \text{Im} \left[\int_M^\infty d\mathcal{E} \frac{1}{E_f - \varepsilon_n - \mathcal{E} + i\eta} T_n^{\mu\mu}(\mathcal{E}, E_f - \varepsilon_n) \right] , \quad (16)$$

where

$$T_n^{\mu\mu}(\mathcal{E}, E) = \lambda_n \langle \varphi_n | j^{\mu\dagger}(\mathbf{q}) \sqrt{1 - \mathcal{V}'(E)} | \tilde{\chi}_{\mathcal{E}}^{(-)}(E) \rangle \langle \chi_{\mathcal{E}}^{(-)}(E) | \sqrt{1 - \mathcal{V}'(E)} j^\mu(\mathbf{q}) | \varphi_n \rangle . \quad (17)$$

In Ref. [22] we have shown that the factor $\sqrt{1 - \mathcal{V}'(E)}$ accounts for interference effects between different channels and allows the replacement of the mean field \mathcal{V} with the phenomenological optical potential \mathcal{V}_L . In Eq. (17) $\mathcal{V}'(E)$ is the energy derivative of the mean field potential. After calculating the limit for $\eta \rightarrow +0$ Eq. (17) reads

$$W^{\mu\mu}(\omega, q) = \sum_n \left[\text{Re} T_n^{\mu\mu}(E_f - \varepsilon_n, E_f - \varepsilon_n) - \frac{1}{\pi} \mathcal{P} \int_M^\infty d\mathcal{E} \frac{1}{E_f - \varepsilon_n - \mathcal{E}} \text{Im} T_n^{\mu\mu}(\mathcal{E}, E_f - \varepsilon_n) \right] , \quad (18)$$

where \mathcal{P} denotes the principal value of the integral. Eq. (18) separately involves the real and imaginary parts of $T_n^{\mu\mu}$.

Let us examine the expression of $T_n^{\mu\mu}(\mathcal{E}, E)$ at $\mathcal{E} = E = E_f - \varepsilon_n$ for a fixed n . This is the most important case since it appears in the first term in the right hand side of Eq. (18), which gives the main contribution. Disregarding the square root correction, due to interference effects, one observes that in Eq. (17) the second matrix element (with the inclusion of $\sqrt{\lambda_n}$) is the transition amplitude for the single nucleon knockout from a nucleus in the state $|\Psi_0\rangle$ leaving the residual nucleus in the state $|n\rangle$. The attenuation of its strength, mathematically due to the imaginary part of \mathcal{V}^\dagger , is related to the flux lost towards the channels different from n . In the inclusive response this attenuation must be compensated by a corresponding gain due to the flux lost, towards the channel n , by the other final states asymptotically originated by the channels different from n . In the description provided by the spectral representation of Eq. (18), the compensation is performed by the first matrix element in the right hand side of Eq. (17), where the imaginary part of \mathcal{V} has the effect of increasing the strength. Similar considerations can be made, on the purely mathematical ground, for the integral of Eq. (18), where the amplitudes involved in $T_n^{\mu\mu}$ have no evident physical meaning as $\mathcal{E} \neq E_f - \varepsilon_n$. We want to stress here that in the Green function approach it is just the imaginary part of \mathcal{V} which accounts for the redistribution of the strength among different channels.

The cross sections and the response functions of the inclusive quasielastic electron scattering are calculated from the single particle expression of the hadron tensor in Eq. (18). After the replacement of the mean field $\mathcal{V}(E)$ by the empirical optical model potential $\mathcal{V}_L(E)$, the matrix elements of the nuclear current operator in Eq. (17), which represent the main ingredients of the calculation, are of the same kind as those giving the RDWIA transition amplitudes of the $(e, e'p)$ reaction. Thus, the same treatment can be used to describe the initial and final state wave functions and the one-nucleon electromagnetic current.

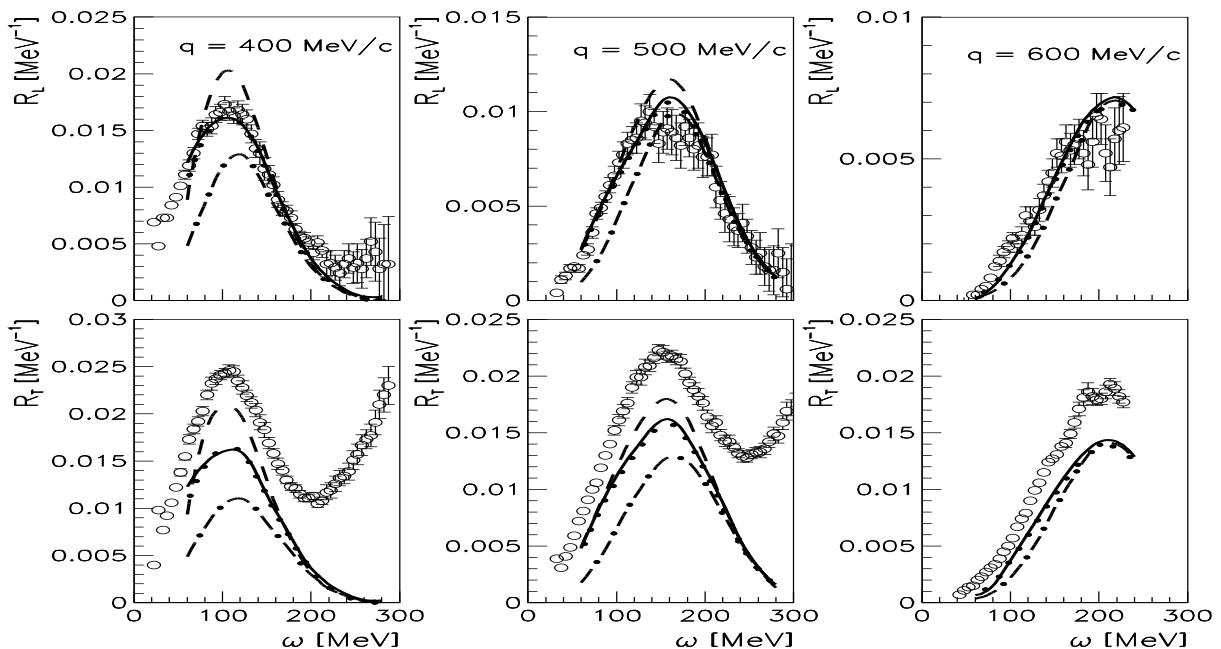


FIG. 4: Longitudinal (upper panel) and transverse (lower panel) response functions for the $^{12}\text{C}(e, e')$ reaction at $q = 400, 500,$ and 600 MeV/c, respectively. Solid and dotted lines represent the relativistic results with and without the inclusion of the factor in Eq. (19), respectively. Dashed lines give the result without the integral in Eq. (18). Dot-dashed lines are the contribution of integrated single nucleon knockout only. The data are from Ref. [40].

A. Results and discussion

The longitudinal and transverse response functions for ^{12}C at $q = 400$ MeV/c are displayed in Fig. 4 (left column) and compared with the Saclay data [40]. The low energy transfer values are not given because the relativistic optical potentials are not available at low energies.

The agreement with the data is generally satisfactory for the longitudinal response. The transverse response is underestimated. This is a systematic result of the calculations and was also found in the nonrelativistic approach of Ref. [41]. It may be attributed to physical effects which are not considered in the single-particle Green function approach, e.g., meson exchange currents.

The effect of the integral in Eq. (18) is also displayed. Its contribution is important and essential to reproduce the experimental longitudinal response.

The contribution arising from interference between different channels gives rise to the factor

$$\sqrt{1 - \mathcal{V}'_L(E)} = \sqrt{1 - \beta S'(E) - V'(E)}. \quad (19)$$

We see, however, that here it gives only a slight contribution, due to a compensation between the energy derivatives $S'(E)$ and $V'(E)$.

The contribution from all the integrated single nucleon knockout channels is also drawn in Fig. 4. It is significantly smaller than the complete calculation. The reduction, which is larger at lower values of ω , gives an indication of the relevance of inelastic channels.

The longitudinal and transverse response functions for ^{12}C at $q = 500$ (middle column) and $q = 600$ MeV/c (right column) are also displayed and compared with the Saclay data [40] in Fig. 4. As already found at $q = 400$ MeV/c, a good agreement with the data is obtained in both cases for the longitudinal response, while the transverse response is underestimated. Only a slight effect is given by the factor in Eq. (19) arising from the interference between different channels. The role of the integral in Eq. (18) decreases increasing the momentum transfer.

In Fig. 5 we consider the $^{16}\text{O}(e, e')$ inclusive cross section data taken at ADONE-Frascati [24] with beam energy ranging from 700 to 1200 MeV and a scattering angle $\vartheta_e \simeq 32^\circ$. The NLSH wave

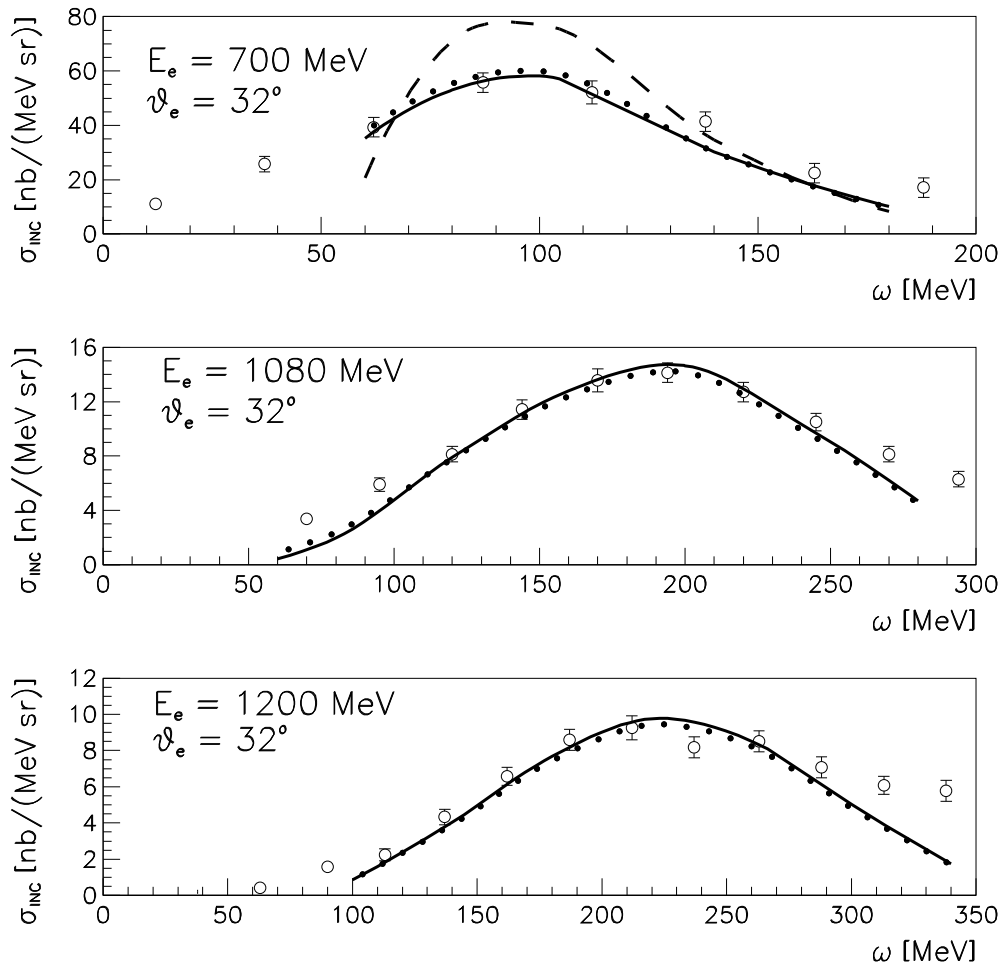


FIG. 5: The cross section for the inclusive $^{16}\text{O}(e, e')$ reaction at $\vartheta_e = 32^\circ$ and $E_e = 700, 1080,$ and 1200 MeV. The data are from ADONE-Frascati [24]. Line convention as in Fig. 4.

functions have been used in the calculations. The agreement with data is good in all the situations considered. The integral in Eq. (18) produces a reduction which is now essential to reproduce the data at 700 MeV, which correspond to a momentum transfer $q \lesssim 400$ MeV/ c . Its contribution can be neglected when $q \simeq 600$ MeV/ c . The effect of the factor in Eq. (19) is very small.

-
- [1] S. Frullani and J. Mougey, *Adv. Nucl. Phys.* **14**, 1 (1984).
 - [2] J. Mougey *et al.*, *Nucl. Phys. A* **262**, 461 (1976).
 - [3] M. Bernheim *et al.*, *Nucl. Phys. A* **375**, 381 (1982).
 - [4] P.K.A. de Witt Huberts, *J. Phys. G* **16**, 507 (1990).
 - [5] L. Lapikás, *Nucl. Phys. A* **553**, 297c (1993).
 - [6] K.I. Blomqvist *et al.*, *Phys. Lett. B* **344**, 85 (1995).
 - [7] M. Leuschner *et al.*, *Phys. Rev. C* **49**, 955 (1994).
 - [8] C. Giusti and F.D. Pacati, *Nucl. Phys. A* **473**, 717 (1987); **A 485**, 461 (1988).
 - [9] S. Boffi, C. Giusti, F.D. Pacati, and M. Radici, *Electromagnetic Response of Atomic Nuclei*, Oxford Studies in Nuclear Physics Vol. 20 (Clarendon Press, Oxford, 1996).

- [10] J.J. Kelly, *Adv. Nucl. Phys.* **23**, 75 (1996).
- [11] A. Picklesimer and J.W. Van Orden, *Phys. Rev. C* **40**, 290 (1989).
- [12] Y. Jin and D.S. Onley, *Phys. Rev. C* **50**, 377 (1994).
- [13] J.M. Udias, J.A. Caballero, E. Moya de Guerra, J.R. Vignote, and A. Escuderos, *Phys. Rev. C* **64**, 024614 (2001).
- [14] M. Hedayati-Poor, J.I. Johansson, and H.S. Sherif, *Phys. Rev. C* **51**, 2044 (1995).
- [15] J.J. Kelly, *Phys. Rev. C* **60**, 044609 (1999).
- [16] A. Meucci, C. Giusti, and F.D. Pacati, *Phys. Rev. C* **64**, 014604 (2001).
- [17] J. Gao *et al.*, *Phys. Rev. Lett.* **84**, 3265 (2000).
- [18] S. Malov *et al.*, *Phys. Rev. C* **62**, 057302 (2000).
- [19] S. Boffi, C. Giusti, F.D. Pacati, and F. Cannata, *Nuovo Cimento A* **98**, 291 (1987).
- [20] A. Meucci, *Phys. Rev. C* **65**, 044601 (2002).
- [21] M. Radici, A. Meucci, and W.H. Dickhoff, *Eur. Phys. J. A* **17**, 65 (2003).
- [22] A. Meucci, F. Capuzzi, C. Giusti, and F.D. Pacati, *Phys. Rev. C* **67**, 054601 (2003).
- [23] C.F. Williamson *et al.*, *Phys. Rev. C* **56**, 3152 (1997).
- [24] M. Anghinolfi *et al.*, *Nucl. Phys. A* **602**, 405 (1996).
- [25] J.P. Chen, S. Choi, and Z.E. Meziani, spokespersons, JLab experiment E-01-016.
- [26] V. Van der Sluys, J. Ryckebusch, and M. Waroquier, *Phys. Rev. C* **51**, 2664 (1995).
- [27] R. Cenni, F. Conte, and P. Saracco, *Nucl. Phys. A* **623**, 391 (1997).
- [28] J.E. Amaro, M.B. Barbaro, J.A. Caballero, T.W. Donnelly, and A. Molinari, *Phys. Rep.* **368**, 317 (2002); *Nucl. Phys. A* **723**, 181 (2003).
- [29] A. Fabrocini, *Phys. Rev. C* **55**, 338 (1997).
- [30] G. Co’ and A.M. Lallena, *Ann. Phys.* **287**, 101 (2001).
- [31] W. Leidemann and G. Orlandini, *Nucl. Phys. A* **506**, 447 (1990).
- [32] I. Sick, in *Nuclear Theory - Proceedings of the XXI International Workshop on Nuclear Theory*, edited by V. Nikolaev (Heron Press Science Series, Sofia, 2002), p. 16.
- [33] G.A. Lalazissis, J. König, and P. Ring, *Phys. Rev. C* **55**, 540 (1997).
- [34] E.D. Cooper, S. Hama, B.C. Clark, and R.L. Mercer, *Phys. Rev. C* **47**, 297 (1993).
- [35] T. de Forest, Jr., *Nucl. Phys. A* **392**, 232 (1983).
- [36] A. Meucci, C. Giusti, and F. D. Pacati, *Phys. Rev. C* **66**, 034610 (2002).
- [37] M.J. Dekker, P.J. Brussaard, and J.A. Tjon, *Phys. Rev. C* **49**, 2650 (1994).
- [38] G.H. Martinus, O. Scholten, and J.A. Tjon, *Phys. Rev. C* **58**, 686 (1998).
- [39] R.J. Woo *et al.*, *Phys. Rev. Lett.* **80**, 456 (1998).
- [40] P. Barreau *et al.*, *Nucl. Phys. A* **402**, 515 (1983); Note CEA N-2334.
- [41] F. Capuzzi, C. Giusti, and F.D. Pacati, *Nucl. Phys. A* **524**, 681 (1991).